PERGAMON

International Journal of Heat and Mass Transfer 43 (2000) 2141–2154

International Journal of HEAT and MASS TRANSFER

www.elsevier.com/locate/ijhmt

Numerical modeling of microwave induced natural convection

Qiong Zhang, Tom H. Jackson, Aydin Ungan*

Department of Mechanical Engineering, Purdue School of Engineering and Technology at Indianapolis, IUPUI, 723 West Michigan Street, Indianapolis, IN 46202, USA

Received 23 March 1999; received in revised form 9 September 1999

Abstract

A three-dimensional numerical model is developed to predict the distribution of electromagnetic fields, power distributions, temperatures, and velocities within a containerized liquid located in a microwave cavity. A three-dimensional Finite-Difference-Time-Domain (FDTD) scheme is used to determine electromagnetic fields and absorbed power by solving the transient Maxwell's equations, and the Finite Control Volume method with SIMPLER algorithm is used to obtain unsteady temperature profiles and flow patterns. Temperature dependence of liquid dielectric properties is simulated through an iterative process. Two liquids, distilled water and corn oil, are chosen to illustrate microwave heating phenomena for high and low loss dielectrics, respectively.

1. Introduction

Microwave heating of liquids has been utilized in a wide range of industrial processes [1]. Microwave heating offers numerous advantages such as short start up time, rapid heating, energy efficiency, precise process control, and food products with better nutritional quality [2]. Knowledge of several parameters is required in order to accurately account for all the phenomena which occur in a liquid heated by microwaves. This includes a description of the electromagnetic field and power distributions, together with a prediction of the liquid's local temperature and velocity. For this reason, the transient Maxwell's, Navier–Stokes, and energy equations need to be solved simultaneously. Because of the number and complexity of the equations involved, numerical modeling is the only viable approach to conducting realistic process simulations.

In the past, an incomplete understanding of microwave power distribution inside a cavity, temperature profiles and flow patterns within the liquid has hindered the advancement of this technology. Recently, many excellent studies in this area [3–7] have highlighted the importance of mathematical modeling on understanding the complex physics that arises during microwave heating of solid specimens. Jia et al. [3] developed a three dimensional model to predict the microwave field and power distribution in a microwave cavity which was based on a finite element modeling approach. The disadvantage of this method was that long computational times were required for even medium sized microwave cavities. Liu et al. [5] applied a Finite Difference Time Domain (FDTD) algorithm to three dimen-

* Corresponding author. Tel.: +1-317-274-9711; fax: +1-317-274-9744.

E-mail address: ungan@engr.iupui.edu (A. Ungan).

0017-9310/00/$ - see front matter
PII: S0017-9310(99)00281-1

Nomenclature

C_{pf}	specific heat capacity of the fluid
E_x	electric field component at X-direction
E_y	electric field component at Y-direction
E_z	electric field component at Z-direction
H_x	magnetic field component at X-direction
H_y	magnetic field component at Y-direction
H_z	magnetic field component at Z-direction
H_c	Height of the microwave cavity
H_l	Height of the containerized liquid
g	acceleration due to gravity
k_f	thermal conductivity of the fluid
L_c	Length of the microwave cavity
L_l	Length of the containerized liquid
p	pressure
$q(x, y, z)$	volumetric microwave heat source
T	temperature
T_0	reference temperature
u	x-velocity component
v	y-velocity component
w	z-velocity component
W_c	width of the microwave cavity
W_l	width of the containerized liquid
XYZ	coordinates system of the microwave cavity
xyz	coordinates system of the fluid and the container.

Greek symbols

α	thermal diffusivity
σ	microwave absorptivity
σ_e	electric conductivity
ν	kinematic viscosity of a fluid
ρ_0	liquid density
β	volume thermal expansion coefficient.

sions and investigated heating in a partially loaded microwave cavity. This work demonstrated the significant effects of placing the dielectric material in various locations within the cavity. Clemens and Saltiel [6] made a significant contribution with a two-dimensional numerical model of microwave heating in a solid specimen which accounted for temperature dependent dielectric properties. In our opinion, FDTD seems to be the simplest and most efficient method to predict electromagnetic field distributions and microwave power dissipation. Also, the method developed by Clemens and Saltiel [6] holds the most promise as a means for realistically modeling microwave heating.

Although microwave energy literature is replete with numerical simulations of microwave heating in solid specimens, there are only a few papers on numerical simulations of microwave heating with liquids. Part of the reason may be that analysis of microwave heating in liquids is considerably more challenging due to the presence of fluid motion, leading to the complex interactions of flow fields, local temperature distributions, and microwave fields within the liquid.

Prosetya and Datta [2] studied natural convection in a cylindrical container exposed to a microwave-heating source which was assumed to decay exponentially into the sample. They observed that temperature profiles were almost linear, and the axial temperature was almost uniform. Their numerical results agreed quite well with the experimental data. However, the assumed variation in microwave power is valid only for large sample dimensions and high loss dielectric materials. For small samples, or low loss dielectric loads, the spatial variations of microwave power must be calculated. Ayappa et al. [8] numerically studied two-dimensional natural convection of liquid in a square cavity exposed to traveling plane microwaves at a frequency of 2.45 GHz. They found that the location, intensity, and number of power peaks influence uniformity of temperature in the liquid.

In the study conducted by Ayappa et al. [8] the dielectric material was assumed to be infinitely long, and its dielectric properties were independent of temperature. In the case of microwave heating of containerized liquids, however, these assumptions may not be justified. This is because fluid circulation patterns and electromagnetic field distributions are three-dimensional in nature. In addition, for most lossy dielectric materials, dielectric properties are strongly influenced by temperature. For this reason, interaction between the local microwave energy absorption, temperature, and flow fields must be considered. Ayappa et al. [8] also used a finite element approach to predict electromagnetic fields. As previously mentioned, this method requires long computational times, even for medium size microwave cavities. This would be particularly problematic in situations where electromagnetic fields have to be repeatedly calculated during the heating processes due to temperature dependence of the dielectric properties.

In the following sections, a simplified case of an empty microwave cavity is examined. A containerized liquid is placed in the same cavity. A comparison of

the numerical solutions with the existing analytical solutions is also provided. Finally, the algorithm is applied to two cases of containerized liquids, distilled water and corn oil, in order to illustrate the coupled phenomena of microwave energy absorption, temperatures, and convection driven flows. The algorithm used in this study employs the FDTD method to predict the local microwave power dissipation in the selected liquids. With microwave power as input, transient temperature and flow patterns in these liquids are simulated using the control volume method with the "SIMPLER" algorithm.

2. Numerical modeling of microwave heating

Fig. 1 presents a schematic of the microwave device examined in this study. The device is comprised of a single mode microwave resonant cavity surrounding a container of liquid. Walls of the cavity are assumed to be made of metal which approximates a perfect electrical conductor. The domain for which the electromagnetic field is analyzed includes the entire region enclosed by the walls of the resonant cavity. For temperature and flow fields the computational domain is limited to the region enclosed by the container, which is smaller than the cavity domain (Fig. 1). For the sake of easy identification, two coordinate systems are defined. The system designated by XYZ is used to describe electromagnetic fields within the entire volume of the resonant cavity, and a second coordinate system, xyz, is designated for the purpose of describing the liquid container domain and its associated main variables (i.e. temperature, absorbed power, and flow field variables).

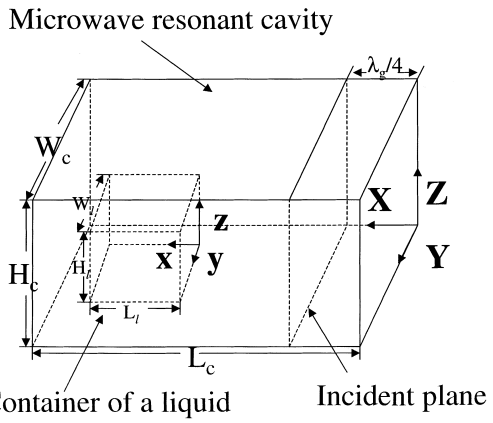

Fig. 1. Schematic of a single-mode microwave resonant cavity and the containerized fluid as the load.

3. Mathematical formulation

Electromagnetic fields within the cavity are defined by Maxwell's equations. The three-dimensional unsteady forms of Maxwell's equations are [9]:

$$\frac{\partial H_X}{\partial t} = \frac{1}{\mu}\left(\frac{\partial E_Y}{\partial Z} - \frac{\partial E_Z}{\partial Y}\right) \tag{1}$$

$$\frac{\partial H_Y}{\partial t} = \frac{1}{\mu}\left(\frac{\partial E_Z}{\partial X} - \frac{\partial E_X}{\partial Z}\right) \tag{2}$$

$$\frac{\partial H_Z}{\partial t} = \frac{1}{\mu}\left(\frac{\partial E_X}{\partial Y} - \frac{\partial E_Y}{\partial X}\right) \tag{3}$$

$$\frac{\partial E_X}{\partial t} = \frac{1}{\epsilon}\left(\frac{\partial H_Z}{\partial Y} - \frac{\partial H_Y}{\partial Z} - \sigma_e E_X\right) \tag{4}$$

$$\frac{\partial E_Y}{\partial t} = \frac{1}{\epsilon}\left(\frac{\partial H_X}{\partial Z} - \frac{\partial H_Z}{\partial X} - \sigma_e E_Y\right) \tag{5}$$

$$\frac{\partial E_Z}{\partial t} = \frac{1}{\epsilon}\left(\frac{\partial H_Y}{\partial X} - \frac{\partial H_X}{\partial Y} - \sigma_e E_Z\right) \tag{6}$$

For boundary conditions, normal components of magnetic fields and tangential components of electric fields are assumed to vanish at the conductive walls. It is worth remarking here that the above equations are valid in the entire resonant cavity, including the air, container, and liquid. Depending upon the substance in a particular region of the domain, the electromagnetic properties may assume different values. Thus, the only boundary conditions needed for the FDTD calculations are those at the cavity walls.

The energy absorption by a lossy dielectric material (in general cases the liquid, and possibly the container) in a microwave field is described by:

$$q(x, y, z) = \sigma \mid E_{\text{rms}} \mid^2 \tag{7}$$

where sigma σ is the temperature dependent absorptivity and E_{rms} is the root mean squared value of the **E** field at a particular location as described by XYZ coordinate system (Fig. 1).

To reduce complexity of the problem, several assumptions have been introduced into the flow and energy equations of the liquid. First, it is assumed that there is no possibility of phase change for the liquid. Additionally, it is assumed the Boussinesq approximation is valid, thus, density of the fluid is assumed constant everywhere except in the body force term. Since the influence of magnetic fields on most liquids is negligibly small, the pondoremotive forces in the

momentum and the contribution of magnetic energy in the energy equation may be neglected. The container is assumed to have heat transfer with ambient air inside the cavity at a fixed temperature. Under these assumptions, the governing equations for the flow and temperature fields in the region as described by xyz coordinates can be written as [10]:

Continuity:

$$\frac{\partial u}{\partial x}+\frac{\partial v}{\partial y}+\frac{\partial w}{\partial z}=0 \tag{8}$$

Momentum equations:

$$\begin{aligned}&\frac{\partial u}{\partial t}+u\frac{\partial u}{\partial x}+v\frac{\partial u}{\partial y}+w\frac{\partial u}{\partial z}\\&\quad=-\frac{1}{\rho_0}\frac{\partial p}{\partial x}+\frac{\partial}{\partial x}\left(\nu\frac{\partial u}{\partial x}\right)+\frac{\partial}{\partial y}\left(\nu\frac{\partial u}{\partial y}\right)\\&\qquad+\frac{\partial}{\partial z}\left(\nu\frac{\partial u}{\partial z}\right)+S_u\end{aligned} \tag{9}$$

$$\begin{aligned}&\frac{\partial v}{\partial t}+u\frac{\partial v}{\partial x}+v\frac{\partial v}{\partial y}+w\frac{\partial v}{\partial z}\\&\quad=-\frac{1}{\rho_0}\frac{\partial p}{\partial y}+\frac{\partial}{\partial x}\left(\nu\frac{\partial v}{\partial x}\right)+\frac{\partial}{\partial y}\left(\nu\frac{\partial v}{\partial y}\right)\\&\qquad+\frac{\partial}{\partial z}\left(\nu\frac{\partial v}{\partial z}\right)+S_v\end{aligned} \tag{10}$$

$$\begin{aligned}&\frac{\partial w}{\partial t}+u\frac{\partial w}{\partial x}+v\frac{\partial w}{\partial y}+w\frac{\partial w}{\partial z}\\&\quad=-\frac{1}{\rho_0}\frac{\partial p}{\partial z}+\frac{\partial}{\partial x}\left(\nu\frac{\partial w}{\partial x}\right)+\frac{\partial}{\partial y}\left(\nu\frac{\partial w}{\partial y}\right)\\&\qquad+\frac{\partial}{\partial z}\left(\nu\frac{\partial w}{\partial z}\right)+S_w-\rho_0 g[1-\beta(T-T_0)]\end{aligned} \tag{11}$$

Energy conservation:

$$\begin{aligned}&\frac{\partial T}{\partial t}+\frac{\partial(uT)}{\partial x}+\frac{\partial(vT)}{\partial y}+\frac{\partial(wT)}{\partial z}\\&\quad=\frac{\partial}{\partial x}\left(\alpha\frac{\partial T}{\partial x}\right)+\frac{\partial}{\partial y}\left(\alpha\frac{\partial T}{\partial y}\right)+\frac{\partial}{\partial z}\left(\alpha\frac{\partial T}{\partial z}\right)\\&\qquad+q(x,y,z)\end{aligned} \tag{12}$$

where S_u, S_v, and S_w stand for source terms other than shown in momentum equations, ν and α are the kinematic viscosity and thermal diffusivity of the liquid, respectively. Again, it should be remarked here that Eqs. (8)–(12) are valid for the liquid as well as the container. However, for the later, since it is solid, the velocities are zero. Eqs. (8)–(12) are subjected to the following boundary conditions. At the liquid–container interfaces, no-slip boundary conditions are used for the momentum equations. At the top surface velocity w and the shear stress in the horizontal directions are assumed to be zero. For the energy equation, the bottom of the container is assumed to be perfectly insulated. At the side walls, heat transfer coefficient through the outside boundary layer are determined from the free-convection heat transfer coefficients. For the top surface, the heat transfer coefficients are selected from free-convection correlation for horizontal flat plates [11].

4. Numerical solution

Eqs. (8)–(12) contain five unknowns: temperature T, velocity components u, v, w, and pressure p. These equations are coupled to the Maxwell equations (Eqs. (1)–(6)) by Equation (7). The later equation represents the heating effect of the microwaves in the liquid–container domain. In accordance with the FDTD method [5,12], the electromagnetic field is calculated using the discretized version of Maxwell's equations. With this method, the electric field components (Es) are stored halfway between the basic nodes while magnetic field components (Hs) are stored at the center [5,12], thus, they are evaluated at alternating half-time steps. In other words, E and H field components are discretized by a central difference method in both spatial and time domains. Eqs. (8)–(12) are solved numerically by using the Finite Control Volume Method along with the SIMPLER algorithm developed by Patankar [13]. Since dielectric properties of most liquids are temperature dependent, to simulate the physics of a microwave heating process realistically it is necessary to consider the coupling between the E field and the temperature distribution. For this reason, the iteration scheme reported earlier [14] is used to resolve the non-linear coupling of Maxwell's equations, Navier–Stokes, and energy equations. Further details about the numerical scheme employed in this paper can be found in [15].

5. Results and discussion

5.1. Model parameters

Two different liquids are simulated in order to illustrate aspects of microwave heating in substances with comparatively high and low dielectric loss factors. Distilled water and corn oil are selected for this purpose. Dimensions of the microwave cavity ($L_c=25.95$ cm $\times$ $W_c=8.65$ cm $\times$ $H_c=6.345$ cm) are selected to satisfy conditions for resonance at 2.45 GHz. Excitation of

the cavity is accomplished by imposing a 2.45 GHz plane polarized source located at $X = 4.2$ cm. Dimensions of the liquid container are selected as $L_l = 6.9$ cm $\times$ $W_l = 5.5$ cm $\times$ $H_l = 3.4$ cm. The distance between origins of the two coordinate systems (Fig. 1) is taken to be $X-x = 0.445L_c$, $Y-y = 0.2W_c$, and $Z-z = 0.001H_c$. It is assumed that the container is full of liquid to the brim and, for simplicity, the liquid's thermal properties are constant. Additionally, dielectric properties of liquids are assumed independent of microwave frequency. The relative dielectric constant and relative dielectric loss factor are obtained by curve fitting third-order polynomials to data reported in [16] for 2.8 GHz microwaves. Thermal and temperature-dependent dielectric properties of the liquids are shown in Table 1.

The container is assumed to be made of a ceramic-based material which is transparent to microwaves at relatively low temperatures (< 100°C). Its thickness is taken to be 2.8 mm with a thermal conductivity of $k_s = 30$ W/m K. The overall heat transfer coefficients for the side walls of the ceramic container are approximated [11] as $U_{side} = 20$ W/m^2. Convective heat transfer coefficients at the top surface of the liquid are obtained from the horizontal flat-plate correlation published in [11]. Initially, the whole calculation domain (air, container, and oil) are assumed to be at a uniform temperature of 297 K. Although the other temperatures are allowed to change with time, the air temperature is assumed to remain constant during the execution.

The dimensionless number commonly used for convection in the presence of a source term is the modified Grashof number which may be defined as [17]:

$$Gr^* = \frac{\rho_0^2 \times g \times \beta \times L_1^5 \times \bar{q}}{\mu^2 \times k} \tag{13}$$

In this study $\bar{q}$ is the volumetrically averaged microwave power density absorbed by the liquid. The computational domain for the entire cavity is divided into a $91 \times 31 \times 23$ array of nodes in X-, Y-, and Z-directions, respectively. The same grid distribution is also utilized for discreticization of the container–liquid (xyz) domain. Systematic trials with various grid sizes revealed that such grid distributions provided grid-independent results with corn oil. However, in simulations with water, more grid nodes ($181 \times 61 \times 46$) are needed because microwave power varies sharply due to water's greater absorptivity of microwave energy.

6. Simulations with the empty cavity

Fig. 2 depicts variations in electric and magnetic field intensity across a plane located at $Z = 0.5H_c$. In the case of an empty microwave cavity, the main point of interest is the distribution of the electric field strength. For this reason the incident electric field is chosen to be 1 V/m with a corresponding magnetic field strength of 1/533.159 V m^{-1} Ω. Additionally, it is assumed that the incident wave has a Transverse Electric (TE) mode. The resulting resonant mode structure shown in Fig. 2 corresponds to a pure TE_{310} mode. The incident plane, located at $X = 4.2$ cm, does not create any discontinuity while the cavity is unloaded.

Fig. 3 provides a comparison of the numerically and analytically predicted rms values of the E and H field components. As shown in Fig. 3, solutions for the electric field are in excellent agreement. In the case of the magnetic field strength some small discrepancies are observed. These may result from the discretization of space and the second-order truncation error created by the FDTD algorithm.

7. Heating simulations with containerized corn oil

The next simulation is performed to examine the characteristics of a cavity loaded with a lossy dielectric liquid. Since the presence of a dielectric material can cause perturbation to the microwave field, regions of high field strength may be shifted. This, in turn, will effect the deposition of energy within the liquid.

Fig. 4 is obtained by assuming constant dielectric

Table 1
Thermal and dielectric properties of the distilled water and corn oil

Properties	Distilled water	Corn oil
ρ_0	1003 kg m^{-3}	920 kg m^{-3}
α	6.1×10^{-4} m^2 s^{-1}	1.9×10^{-4} m^2 s^{-1}
β	5.344×10^{-4} l K^{-1}	3.8×10^{-4} l K^{-1}
ν	6.9×10^{-7} m^2 s^{-1}	6.6×10^{-6} m^2 s^{-1}
C_{pf}	4182.51 J kg^{-1} K^{-1}	2100 J kg^{-1} K^{-1}
ϵ_r'	$-7.2883 \times 10^{-5}T^3 + 0.0057366T^2 - 0.42656T + 84.4515$ (T in °C)	$3.998 \times 10^{-6}T^2 + 0.001313T + 2.587$ (T in °C)
ϵ_r''	$-4.2471 \times 10^{-5}T^3 + 0.0097473T^2 - 0.71507T + 22.9926$ (T in °C)	$1.454 \times 10^{-6}T^2 + 0.00172T + 0.1214$ (T in °C)

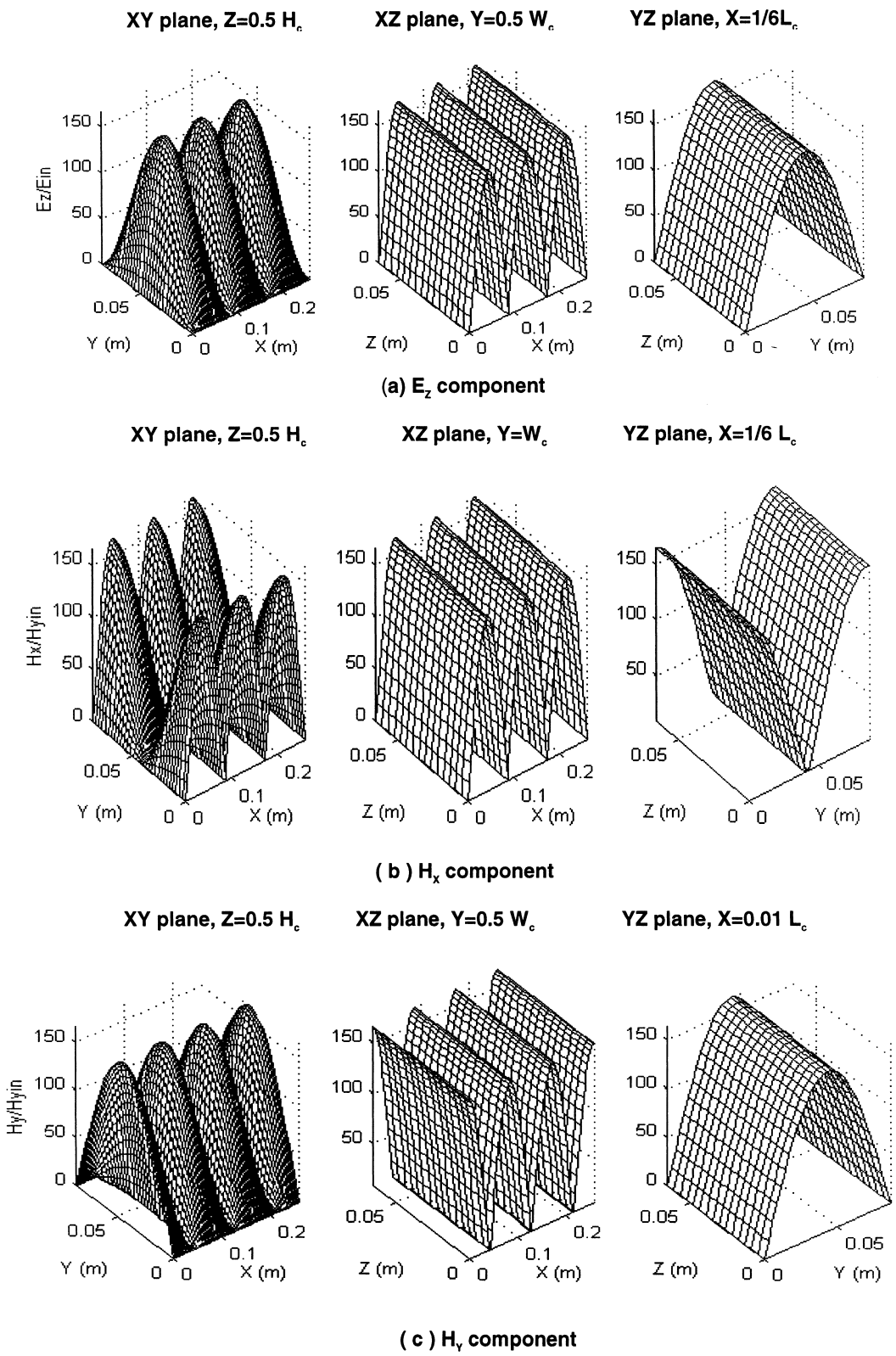

Fig. 2. Distribution of predicted rms values of E and H field components for the empty cavity.

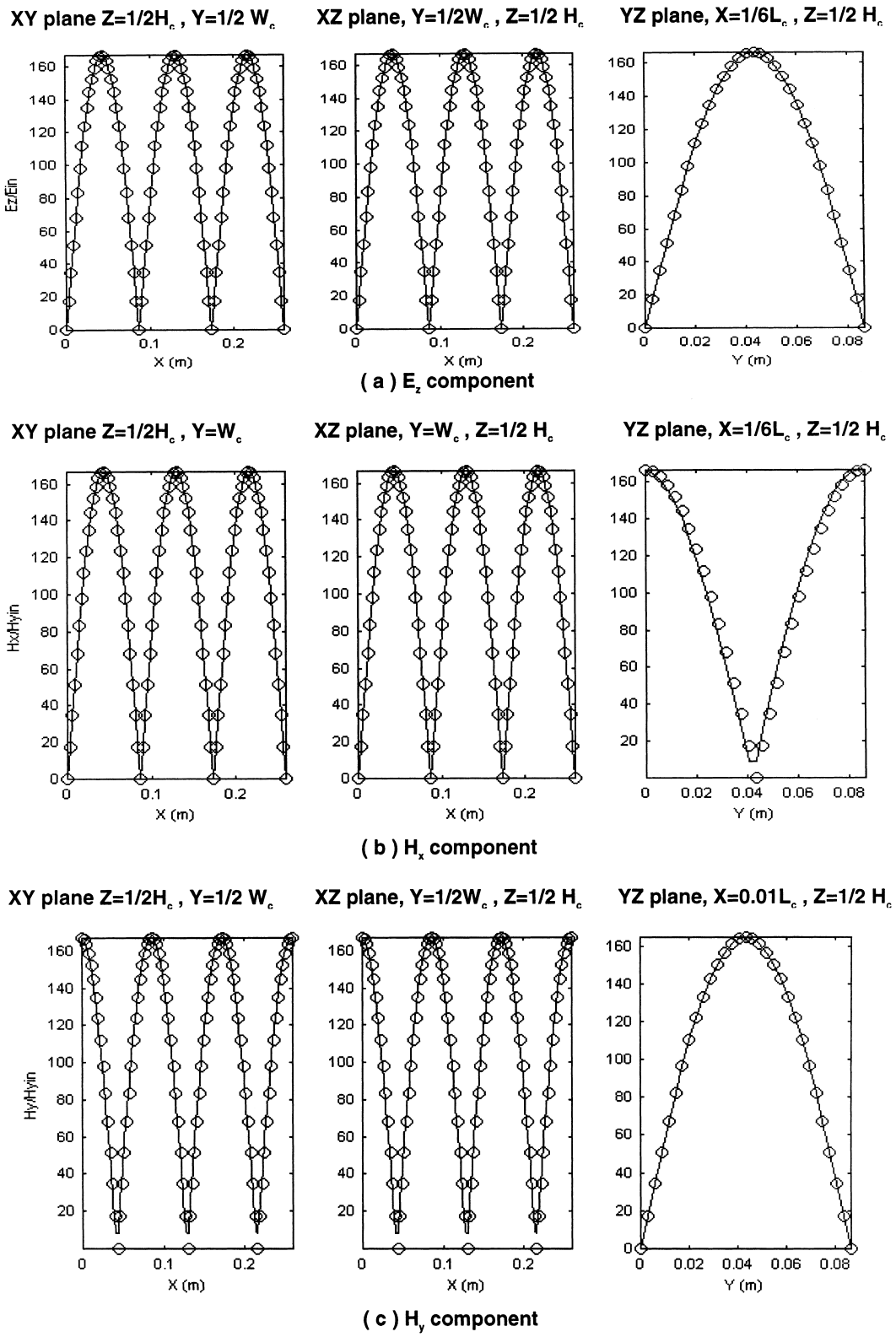

Fig. 3. Comparison of numerical solutions with analytical solutions of field components for TE_{310} mode. "–": numerical solution, "o": analytical solution.

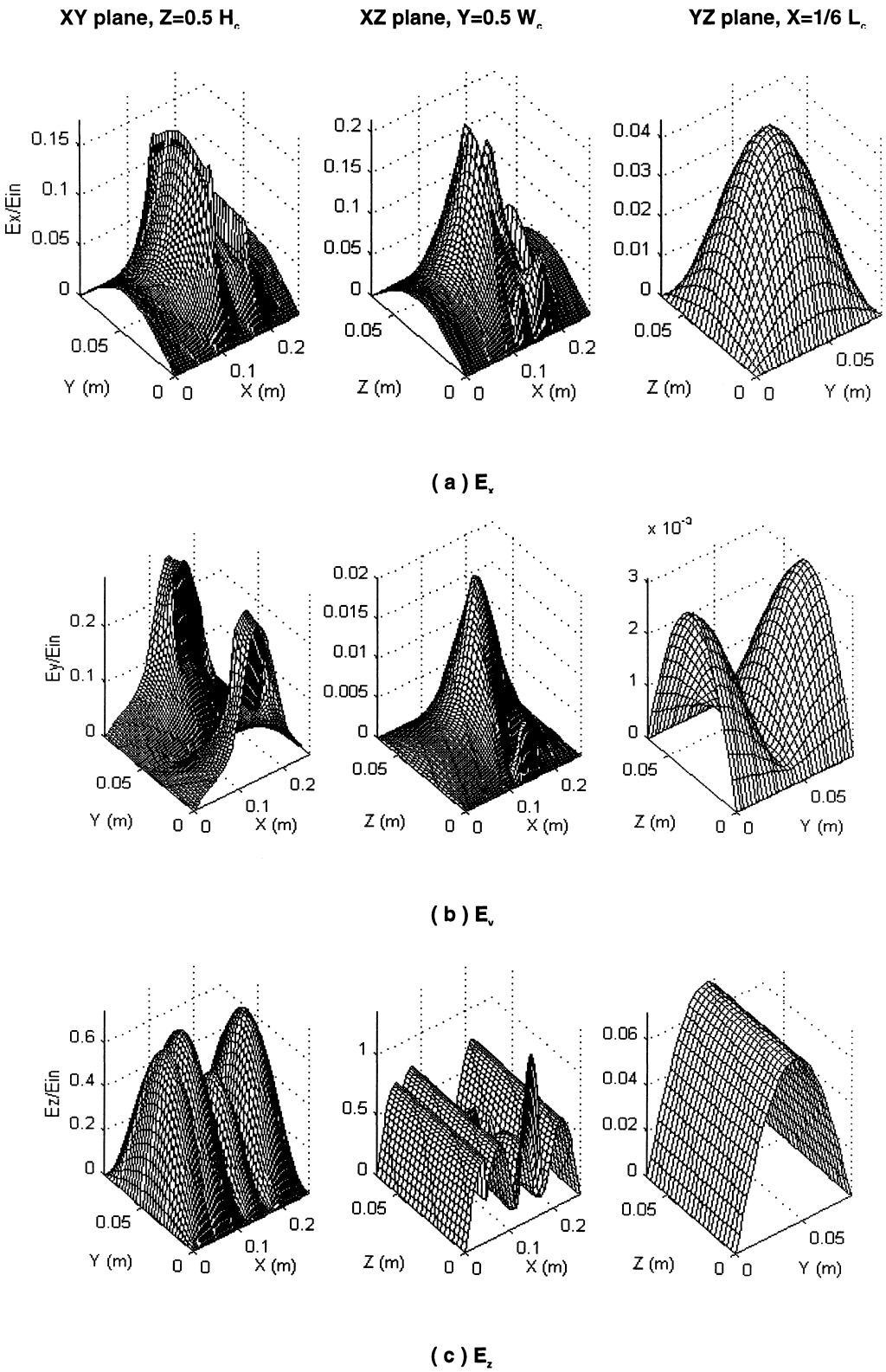

Fig. 4. Distribution of predicted rms values of *E*-field components with dielectric load at the onset of heating (note: temperature distribution is uniform).

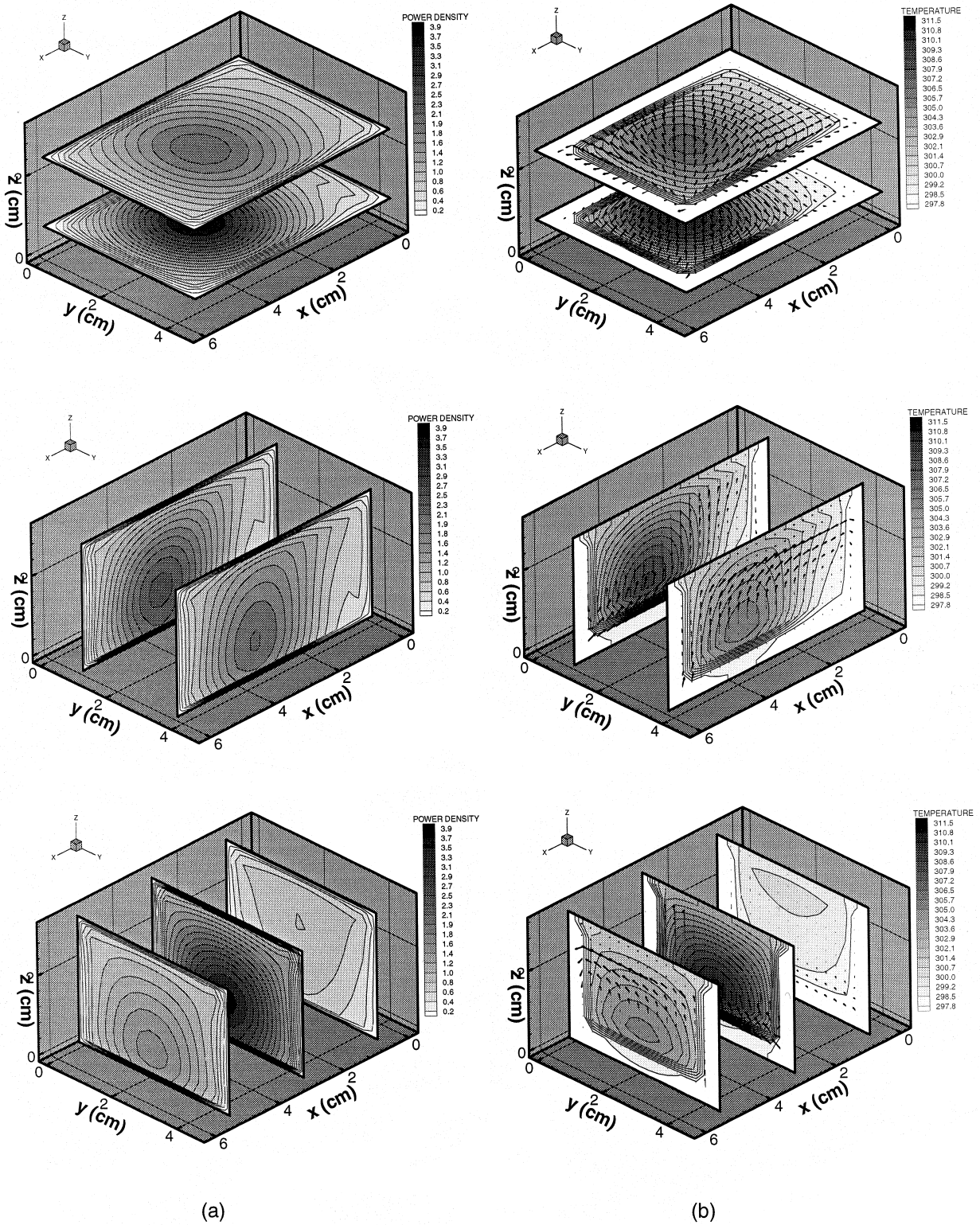

Fig. 5. (a) Power densities (W cm^{-3}) at $t = 0$ s, and (b) temperatures (K) and flow field (cm s^{-1}) patterns at $t = 63$ s in corn oil.

properties throughout the container. This situation corresponds to the transient case where the microwave field is suddenly turned on, but, no temperature change has occurred yet due to thermal inertia. It is observed that the E field has been altered by the presence of the corn oil, not only in the region containing the liquid but in the surrounding cavity as well. Two other phenomena are noteworthy here. First, comparing Fig. 2a with Fig. 4c reveals that the loaded cavity has been excited to a higher TE_{410} mode of resonance, and field components vary along the Z-direction. Second, the appearance of the other two electric field components E_x and E_y shown in Fig. 4a and c reveal that the polarity of the wave had been dramatically changed from a pure TE mode to a hybrid mode. The later mode has both non-zero transverse and longitudinal components. The mode and polarity change significantly moves the region of maximum heating and indicates the importance of three-dimensional simulations. Two-dimensional models simply cannot predict the change of the field polarity, and the variations of field strengths along the Z-direction.

Fig. 5a illustrates the initial absorbed power density distribution at $t = 0$ s. Fig. 5b shows temperature profiles and velocity vectors at time $t = 60$ s for various horizontal (x–y), vertical (x–z), and lateral (y–z) cross-sections, as indicated in the figure. The Gr^* number is about 0.451×10^4, and the Rayleigh number is about 3.5×10^6. At 2.45 GHz the penetration depth of microwaves into oil is about 37.6 cm [8], which is much greater than the typical dimensions of the oil container. Thus, a large portion of the microwaves is able to penetrate through the oil. However, partially due to the difference of dielectric properties between oil and air, and partially due to the internal reflections occurring at the air–container interface, the absorbed power peaks occur near the right of the geometrical center of the container. It should be remarked here that we intentionally placed the container centered in the maxima of the electric field for an empty cavity along the x-direction (Fig. 2). The location of the power peak in the X-direction for the containerized oil in the cavity is $X = 0.533L_c$, a distance shift of $0.033L_c$ (or 8.6 mm) from the location of maxima of the E_z field in an empty cavity $X = 0.5L_c$. In the Y-direction, the shift of power peak location is about 3 mm. The power density at the right edge of the container is found to be higher than at the left side of the oil. This location shift of the maxima and non-symmetrical distribution may result from disturbances of the electromagnetic field in the cavity by the oil/container.

Fig. 5 illustrates the power density distribution (Fig. 5a, the left three depictions) along with the temperature and velocity fields (Fig. 5b, the right three depictions) at various cross sections in the oil container during the early stages of heating. The effect of circulation is virtually negligible so that the microwave absorption occurs in the quiescent oil. Thus, in the absence of circulation, the spatial temperature patterns are mainly determined by the distribution of the microwave power density within the oil. Therefore, the asymmetrical power density creates on asymmetrical temperature distribution. At the lower regions where the heat is primarily transferred by the conduction mode, the asymmetric temperature distribution is more pronounced. Also noteworthy is the presence of a power peak which creates a hot spot, inducing a large circulation cell in the container.

As the heating proceeds, the power density distribution in the oil bath decreases because the electric field strength attenuates as the temperature levels increase. However, circulation becomes stronger and plays a more important role, especially at the upper portion of the oil bath. Fig. 6 depicts the power density distribution (Fig. 6a, the left three illustrations) along with the temperature and velocity fields (Fig. 6b, the right three illustrations) at various cross sections in the oil bath at $t = 183$ s. By comparing Fig. 5a with Fig. 6a, it is seen that power density within the oil has been reduced by a factor of 6, and the power peak has been moved up by about 2 mm. It is noteworthy that circulation cells became more significant, and hot spots had been push up by about 0.6 cm due to convection. The difference between the maximum and the minimum temperature is about 34°. Since the surrounding air temperature remains identical to the initial temperature of oil, the region close to the wall cools down by convection heat transfer from the container wall to the air. Thus, this region remains the coolest area in the oil bath. The variation of the microwave power deposition, temperature and velocity fields at $t = 63$ s and $t = 183$ s fully illustrate the complicated interactions of microwave power, temperature and velocity fields.

8. Simulations with the containerized distilled water

Fig. 7a depicts the distribution of the power density at $t = 0$ s and Fig. 7b shows the temperatures and velocity patterns at $t = 20$ s within a water bath. Since water strongly absorbs microwave energy, an incident microwave with a field strength of 10,000 V m^{-1} is used. The Gr^* number in this case is about 0.671×10^4 while the Rayleigh number is in the vicinity of about 4.578×10^4. As expected, since the microwave penetration depth is about 0.017 m (smaller than the dimensions of the container), most of the microwave energy is absorbed by water. For this reason, the power density decays along the x-direction in which the incident microwave propagates, giving rise to con-

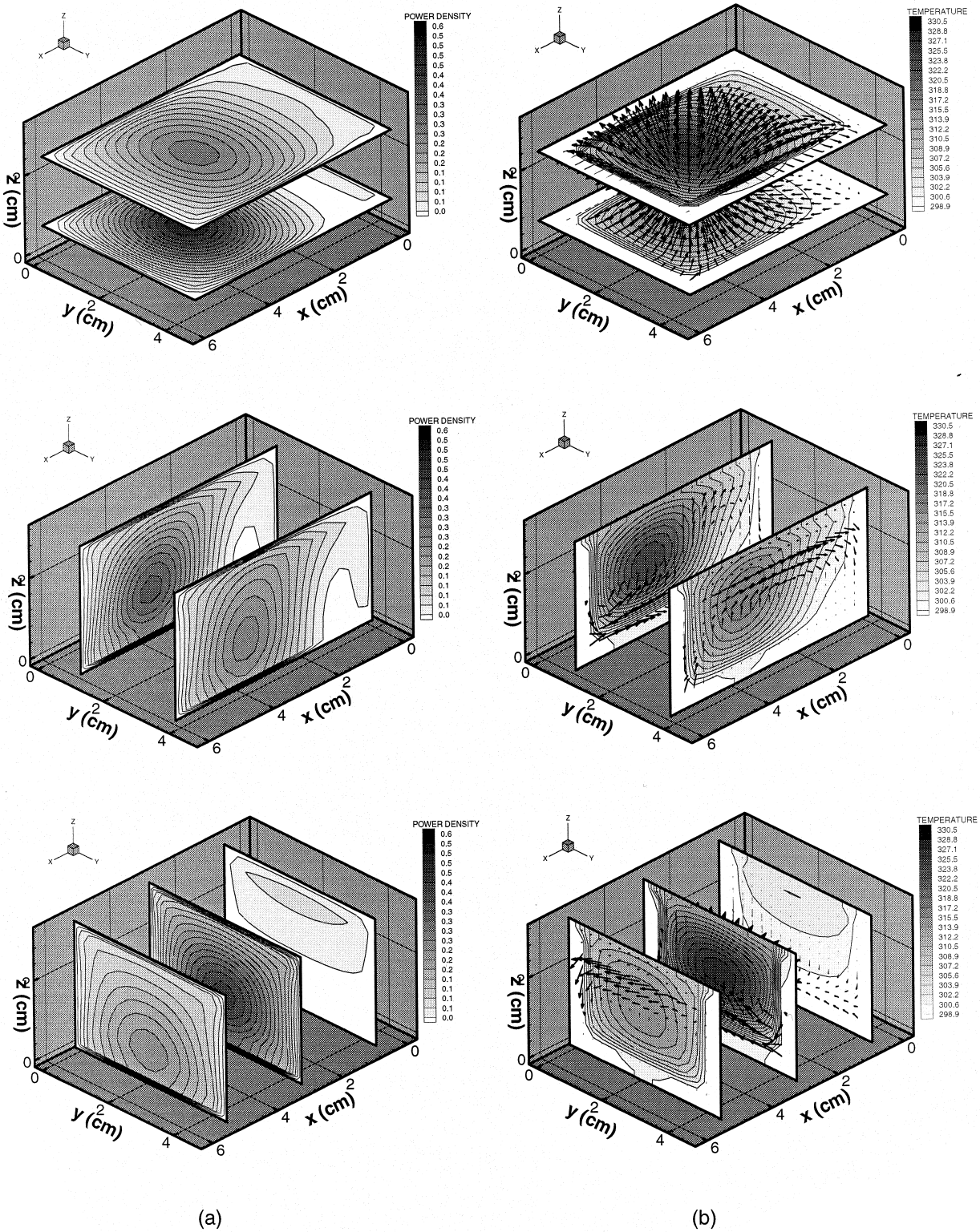

Fig. 6. (a) Power densities (W cm^{-3}) at t = 183 s, and (b) temperatures (K) and flow field (cm s^{-1}) patterns at t = 183 s in corn oil.

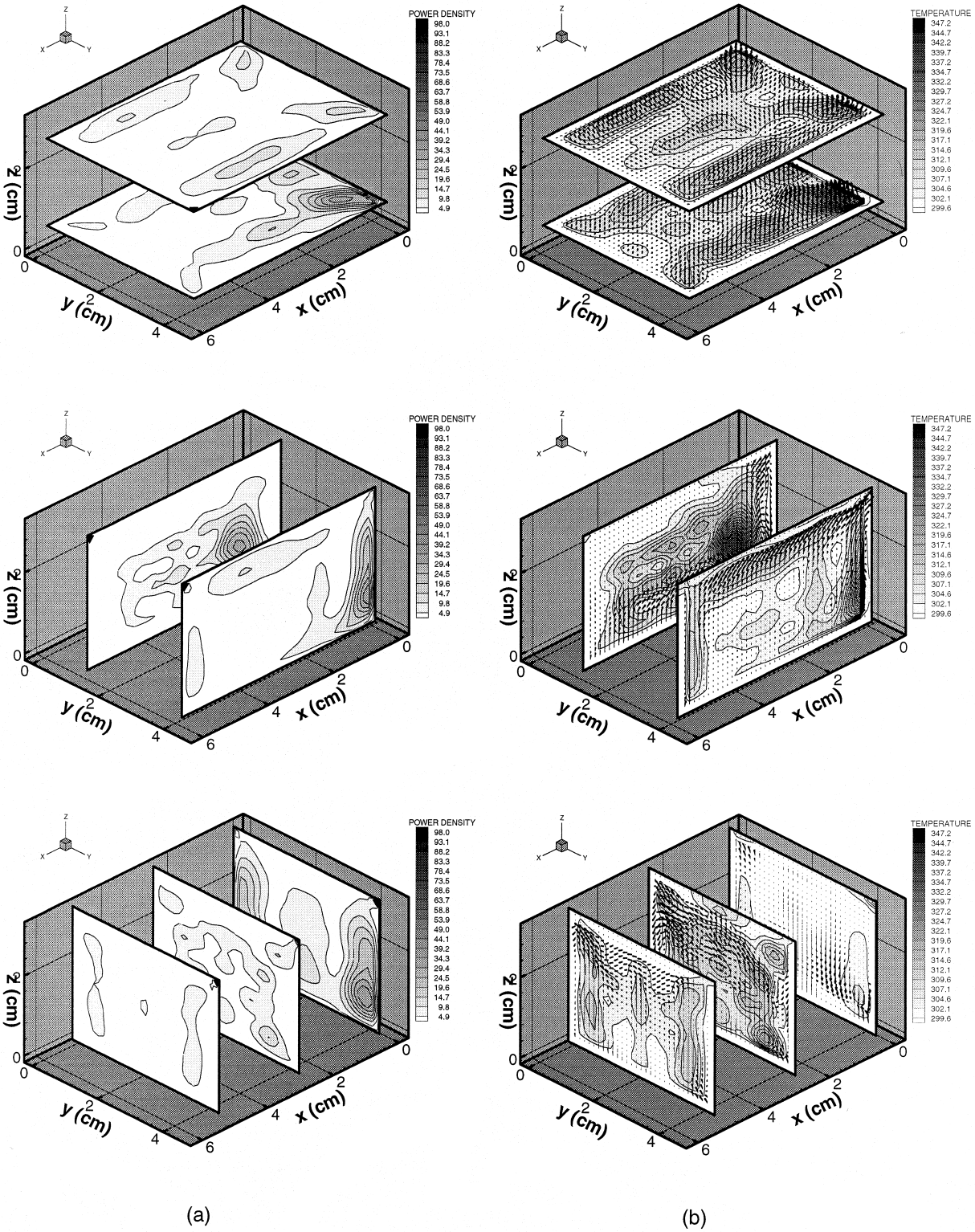

Fig. 7. (a) Power densities (W cm^{-3}) at $t = 0$ s, and (b) temperatures (K) and flow field (cm s^{-1}) patterns at $t = 63$ s in distilled water.

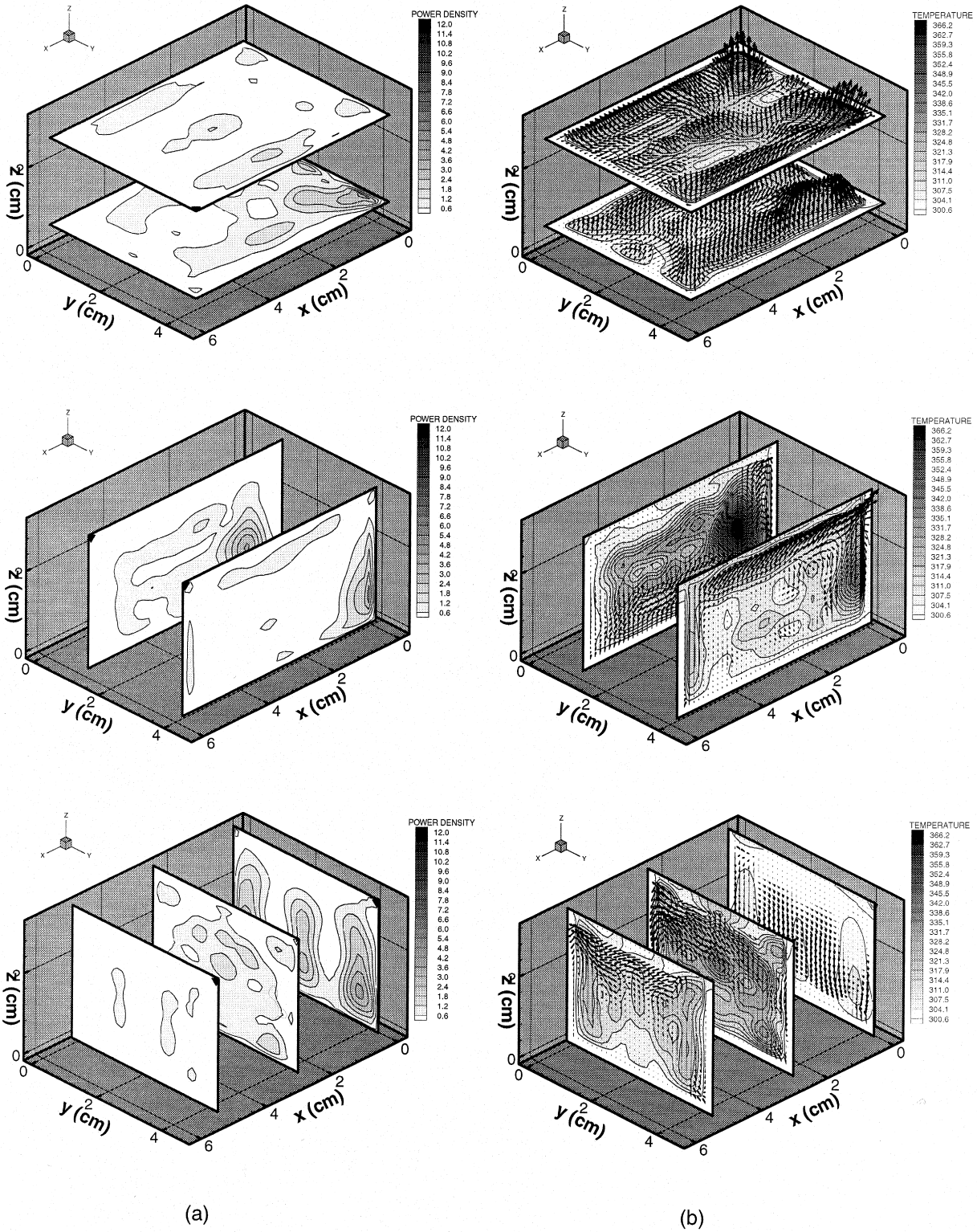

Fig. 8. (a) Power densities (W cm^{-3}) at t = 183 s, and (b) temperatures (K) and flow field (cm s^{-1}) patterns at t = 183 s in distilled water.

centration of hot spots and convection cells at the side of the container closest to the microwave source. This is quite different than the corn oil in which the power peak is located closer to the wall.

As time proceeds temperature increases which, in the case of water, reduces the absorption coefficient, giving rise to decreased energy absorption. Fig. 8 shows the power density, temperature and velocity patterns at the end of heating when $t = 183$ s. The reduction in absorption coefficient and dielectric constant values has significantly altered the power density patterns. This variation in the altered power density once more emphasizes the importance of using an iterative procedure [6,14,15]. In such methodology, dielectric properties are implemented as a function of temperature in the algorithm. As with the corn oil, when the temperature of the water increases, convection is more pronounced. As a result, temperature gradients are reduced. Also, the temperature at the top portion of the water increases. It can be seen that temperatures near the middle of the water container tend to be uniform because hot spots have moved upwards. At the area near the bottom of the walls where convection is quite weak, temperature distributions are still dominated by the microwave heating source. For this reason, temperatures vary greatly throughout the container region.

9. Conclusions

To illustrate the merits of this model, simulations are performed on microwave heating of corn oil and distilled water. Temperature dependence of dielectric properties of these two liquids is accounted for. The results reveal complicated interaction between the electromagnetic fields, energy and flow fields. The transient distribution of absorbed power, temperature and velocity fields illustrate the difference of heating a liquid and heating of solid. In heating of liquid, convection plays a significant role on the distribution of temperature. The numerical methodology reported in this paper provides a tool to design microwave cavities for applications such as heating, drying or cooking purposes where the primary concern is uniform and rapid heating.

References

[1] A.C. Metaxas, R.J. Meridith, Industrial Microwave Heating, Peter Peregrinus Ltd, London, 1983.

[2] H. Prosetya, A. Datta, Batch microwave heating of liquids: an experimental study, Journal of Microwave Power and Energy 26 (4) (1991) 215–226.

[3] X. Jia, M. Bialkowski, Simulation of microwave field and power distribution in a cavity by a three dimensional finite element method, Journal of Microwave Power and Electromagnetic Energy 27 (1992) 11–22.

[4] Deepak, J.W. Evans, Calculation of temperatures in microwave-heated two-dimensional ceramic bodies, Journal of American Ceramic Society 76 (8) (1993) 1915–1923.

[5] F. Liu, I. Turner, M. Bialkowski, A finite-difference time-domain simulation of power density distribution in a dielectric loaded microwave cavity, Journal of Microwave Power and Electromagnetic Energy 29 (3) (1994) 138–147.

[6] J. Clemens, C. Saltiel, Numerical modeling of materials processing in microwave furnaces, International Journal of Heat and Mass Transfer 39 (8) (1996) 1665–1675.

[7] F. Xiao, Y. Hatsuo, Numerical dispersion relation of FDTD method in general curvilinear coordinates, IEEE Microwave and Guided Wave Letters 7 (2) (1997) 48–50.

[8] K.G. Ayappa, S. Brandon, et al., Microwave driven convection in a square cavity, AIChE Journal 40 (7) (1994) 1268–1272.

[9] P.O. Gandhi, Microwave Engineering and Applications, 1st ed., Pergamon Press Inc, New York, 1981.

[10] R.L. Panton, Incompressible Flow, 2nd ed., John Wiley and Sons Inc, New York, 1996.

[11] F. Incropera, D. Dewitt, Fundamentals of Heat and Mass Transfer, 3rd ed., John Wiley and Sons Inc, New York, 1996.

[12] K. Kunz, R. Luebbers, Finite Difference Time Domain Method for Electromagnetics, 1st ed., CRC Press, Boca Raton, 1993.

[13] S.V. Patankar, Numerical Heat Transfer and Fluid Flow, Hemisphere Publishing Corporation, New York, 1980.

[14] Q. Zhang, T. Jackson, A. Ungan, Numerical simulation of continuous microwave hybrid heating process, HTD-Vol. 351, Proceedings of the ASME Heat Transfer Division 1 (1997) 35–41.

[15] Q. Zhang, Parametric study of heating of a containerized liquid in a single-mode microwave cavity, MS thesis, Indiana University–Purdue University at Indianapolis, IN, 1998.

[16] N.E. Bengtsson, P.O. Risman, Dielectric properties of foods at 3 GHz as determined by a cavity perturbation technique, Journal of Microwave Power 6 (2) (1971) 107–123.

[17] D.K. Gartling, A finite element analysis of volumetrically heated fluids in an axisymemetric enclosure, in: R.H. Gallagher (Ed.), Finite Element in Fluids, Wiley, New York, 1982.